Earth and Planetary Science Letters 562 (2021) 116858

Contents lists available at ScienceDirect

Earth and Planetary Science Letters

www.elsevier.com/locate/epsl

Qinghai-Tibet Plateau wetting reduces permafrost thermal responses to climate warming

Guofei Zhang [a], Zhuotong Nan [a,b,*], Lin Zhao [c], Yijia Liang [a], Guodong Cheng [d]

[a] Key Laboratory of Ministry of Education on Virtual Geographic Environment, Nanjing Normal University, Nanjing 210023, China
[b] Jiangsu Center for Collaborative Innovation in Geographical Information Resource Development and Application, Nanjing 210023, China
[c] School of Geographical Sciences, Nanjing University of Information Science & Technology, Nanjing 210044, China
[d] Northwest Institute of Eco-Environment and Resources, Chinese Academy of Science, Lanzhou 730000, China

ARTICLE INFO

Article history:
Received 16 October 2020
Received in revised form 25 February 2021
Accepted 26 February 2021
Available online 10 March 2021
Editor: Y. Asmerom

Keywords:
climate wetting
permafrost
thermal regime
numerical modeling
Qinghai-Tibet Plateau

ABSTRACT

Permafrost, as one of the cryospheric indicators, is extremely sensitive to climatic changes. The Qinghai-Tibet Plateau has experienced remarkable warming and wetting since the mid-1990s. Its recent wetting alters thermal and hydrological properties in permafrost regions and inevitably affects permafrost thermal dynamics. While previous studies mostly focused on the effects of warming on permafrost, little attention has been paid to the effects of concomitant wetting. Here, a land surface model adapted for permafrost simulation is employed to quantitatively investigate the impacts of climate warming and wetting on permafrost thermal regimes by setting up a group of hypothetical numerical scenarios on the basis of historical meteorological records. The results reveal that climate wetting reduces permafrost thermal responses to warming and this effect is especially evident in the arid and semi-arid zones. It was estimated that one-degree warming induces an average increase of 0.46 m in active layer thickness (ATL) and 0.53 °C in temperature at the top of permafrost (TTOP), and a 100 mm wetting in summer precipitation leads to a mean decrease of 0.35 m in ALT and 0.36 °C in TTOP. Furthermore, we found through the simulations that increased summer precipitation imposes dual effects on permafrost in semi-arid high altitudes.

1. Introduction

Permafrost is one of the key components of the terrestrial system, which provides both positive and negative feedbacks to the climate systems (Cheng, 2004; Koven et al., 2011; Zimov et al., 2006). It was reported in Intergovernmental Panel on Climate Change (IPCC) Fifth Assessment Report that the period of 1983–2012 was very likely the warmest 30-year period in the last 800 years and likely the warmest 30-year period in the last 1400 years in the Northern Hemisphere (IPCC, 2013). The Qinghai-Tibet Plateau (QTP) is the highest and most extensive permafrost region in mid-latitudes across the world, and it is considered to be one of the most sensitive areas to global climate change (Liu and Chen, 2000; Yao et al., 2012). Both observations and simulation studies indicate that the QTP has experienced prominent warming since the 1980s (Kuang and Jiao, 2016; Niu et al., 2004). As a result, substantial degradation of permafrost has been observed on the QTP (Cheng et al., 2019; Cheng and Wu, 2007; Kang et al., 2010). Meanwhile, in recent decades, both warming and concomitant wetting on the QTP were recorded (Gao et al., 2014; Li et al., 2010). Meteorological research shows that the QTP has become wetter as a whole since the 1980s, although there still exist large variabilities in space. For example, annual precipitation (AP) has decreased in the southern and eastern QTP and increased in the central part (Yang et al., 2014; Zhang et al., 2017; Zhong et al., 2011; Zhou et al., 2019). The wetting climate has been most pronounced since the mid-1990s. Thousands of lakes on the QTP have been expanding due to increased precipitation (Lei et al., 2014; Yang et al., 2018). The wetting pattern has a strong positive correlation to increasing precipitation, with a correlation coefficient of up to 0.97 (Gao et al., 2015). The Community Climate System Model projected a general wetting trend over the entire QTP, with the greatest increase in the occurrence frequency of heavy precipitation. The wetting was projected to be stronger under the Representative Concentration Pathway (RCP) 8.5 than RCP 4.5 along with an increase in temperature (Gao et al., 2017). The coexistence of both warming and wetting processes and their interactions exert substantial influences on permafrost thermal responses to climate change on the QTP. Therefore, it raises important questions about

* Corresponding author at: Key Laboratory of Ministry of Education on Virtual Geographic Environment, Nanjing Normal University, Nanjing 210023, China.
E-mail address: nanzt@njnu.edu.cn (Z. Nan).

https://doi.org/10.1016/j.epsl.2021.116858

how warming and wetting jointly affect permafrost thermal dynamics on the QTP, and what are the distinct roles of separated warming and wetting processes under this warming-wetting context.

Previous studies have mostly focused on the impacts of climate warming on permafrost changes and concluded that underway permafrost degradation was primarily driven by regional warming climate (Biskaborn et al., 2019; Cheng et al., 2019; Ran et al., 2018; Yao et al., 2019). However, the effects associated with the changing precipitation over the QTP cannot be neglected, as precipitation may greatly impact the freeze-thaw cycle within the active layer and modify thermal dynamics within permafrost. In recent periods, precipitation was reported to increase in high altitudes and arid areas, and to decline in wet regions (Gao et al., 2015). At high altitudes, changing precipitation may play an important role in altering permafrost thermal regimes alongside warming temperature. To date, only a limited number of studies have investigated the effects of wetting on permafrost dynamics. Recently, a relevant study found that an increase in year-around precipitation triggered a cooling effect in the active layer in frozen seasons and a heating effect in thawed seasons (Li et al., 2019). Permafrost monitoring has indicated that increased summer precipitation spells critical impacts for deepening active layer thickness (ALT) (Wu et al., 2015). In another observational study, the increase in precipitation was closely connected to the reduction in ground surface temperature and slowing permafrost degradation (Cai et al., 2018). A study of precipitation extremes suggests precipitation impeded the rising rate of permafrost temperature (Zhu et al., 2017). The rainfall during summers may cool down the active layer such that increased rainfall may mitigate permafrost degradation (Wen et al., 2014). Those studies consistently suggest that wetting has the potential to reduce permafrost warming and potentially mitigate its degradation. However, due to the sparse distribution and limited representativeness of the monitoring sites, they may not be representative of the entire plateau that has a vast area and complex terrain. Consequently, it is imperative to quantitatively assess, through a modeling approach, the effects of wetting on the thermal dynamics of permafrost over the entire QTP.

In this study, we aim to quantify the impacts of warming and wetting on permafrost thermal regimes using a water-heat coupled land surface model (LSM) through numerical experiments to account for various warming and/or wetting scenarios. First, we analyzed the spatiotemporal changes in air temperature and precipitation between two periods, i.e., 1983–1997 and 1998–2012. Then, we assessed permafrost responses to warming and wetting conditions by contrasting the scenarios representing different warming/wetting conditions with a control scenario that represents no warming and wetting trends between two study phases. Finally, we investigated the potential mechanism of the effects of wetting on permafrost dynamics.

2. Methods

The Noah LSM has long been widely used by the United States National Center for Environmental Prediction to provide land surface parameters for regional climate systems. It integrates the Penman-Monteith equation, multi-layer soil model, canopy evapotranspiration formula (Mahrt and Ek, 1984), and later a simple water balance model, and snow and frozen soil parameterization schemes (Chen et al., 1997; Ek et al., 2003). Many studies have confirmed the capability of Noah LSM in simulating thermal and hydrological processes of frozen ground (Chen et al., 2010, 2015; van der Velde et al., 2009; Wu et al., 2018; Zheng et al., 2017).

The model used in this study is a modified version of Noah LSM 3.4.1 (Wu et al., 2018), with special treatments for permafrost simulation, including a modified thermal roughness scheme for sparse vegetation and improved parameterization of thermal and hydraulic conductivities to account for gravel and ground-ice content. The details of the modeling procedure, as used in the present study, were presented by Zhang et al. (2019). A scenario-based numerical simulation approach was developed to quantify the impacts of climate warming and wetting on permafrost. The experiment consists of four scenarios: a control scenario (CTL) representing no warming and wetting trends between two stages, three comparative scenarios representing warming and wetting combinations, i.e., warming alone, wetting alone, and historical (indicating both warming and wetting). The historical scenario was built upon the China Meteorological Forcing Dataset (CMFD) (Chen et al., 2011; He et al., 2020), which provides long term reanalyzed time series of seven atmospheric variables at a 3hr time step. It represents the real warming and wetting climate conditions, under which permafrost changes over the QTP have occurred. The resting scenarios were constituted by intentionally modifying air temperature and precipitation data while retaining the other atmospheric variables in the historical scenario. By contrasting the outcomes of the warming/wetting scenarios and the CTL, the impacts of warming/wetting on permafrost can be identified.

Gao et al. (2014) reported an abrupt change in annual air temperature and precipitation over the QTP around 1998. A similar break point was also detected from the CMFD. Therefore, we divided the entire study period from 1983 to 2012 into two phases preceding and succeeding 1998, with 1998 as the pivotal year. The dataset covering the entire study period was separated into two parts, i.e., pre- (1983–1997) and post- (1998–2012) phases. The temperature time series was broken up into two segments: T_{pre} and T_{post}, denoting temperature data in pre-phase and post-phase, respectively. Since historical air temperatures were increasing through the entire period, T_{pre} and T_{post} are able to represent low and high levels of air temperature that have already occurred, respectively. Likewise, precipitation data were separated into P_{pre} and P_{post} for the two phases. P_{post} represents a condition of more precipitation than P_{pre}. As shown in Table 1, three hypothetical scenarios were created by assembling different temperature and precipitation segments for the two phases while keeping other driving variables unchanged. The CTL that assumes no changes between the two phases has temperature and precipitation data in the post-phase identical to the counterparts in the pre-phase. The warming alone scenario duplicates the historical scenario except that precipitation in the post-phase is replaced by the counterpart in the pre-phase. Because T_{post} is warmer than T_{pre}, the warming alone scenario simulates an exclusively warming condition. Similarly, the wetting alone scenario constrains temperatures in the post-phase identical to the pre-phase and retains natural precipitation.

Because all scenarios have the same temperature and precipitation conditions in the pre-phase on purpose, we focused on the outcomes in the post-phase. The CTL outcomes can serve as a contrast benchmark as there are no phase-wide variations in temperature and precipitation between the pre- and post-phase. By contrasting the simulation results from the warming/wetting scenarios to the CTL, the impacts of warming and wetting and their sole contributions can be determined. Permafrost dynamics from 1983 to 2012 were simulated for the four scenarios by the modified Noah LSM after a 32-year spin-up, for which the years 1979–1982 are used. The temporal and spatial resolutions are 3 hr and $0.1^\circ \times 0.1^\circ$, respectively. The modeling depth amounts to 15.2 m with 18 soil layers. The changes were measured in terms of some key thermal indicators for permafrost, which include ALT, temperature at the top of permafrost (TTOP), and permafrost area. Specifically, a grid cell is identified as underlying permafrost where the maximum monthly mean temperature remains below 0 °C for over 24 months in at least one soil layer as per the definition

Table 1
Setup of scenarios by assembling air temperature and precipitation segments extracted from the historic records.

Scenarios	Scenario segments	
	Pre-phase (1983–1997)	Post-phase (1998–2012)
Control (CTL)	T_{pre}–P_{pre}	T_{pre}–P_{pre}
Warming alone	T_{pre}–P_{pre}	↑T_{post}–P_{pre}
Wetting alone	T_{pre}–P_{pre}	T_{pre}–P_{post}↑
Historical (both warming and wetting)	T_{pre}–P_{pre}	↑T_{post}–P_{post}↑

Note: The control, warming alone, and wetting alone scenarios are hypothetical. Temperature segments, T_{pre} and T_{post}, and precipitation segments, P_{pre} and P_{post}, are extracted from the historical records. The subscripts, pre and post, represent the segments from pre-phase and post-phase, respectively. The symbol ↑ denotes a higher temperature/precipitation condition compared to the counterpart in the CTL.

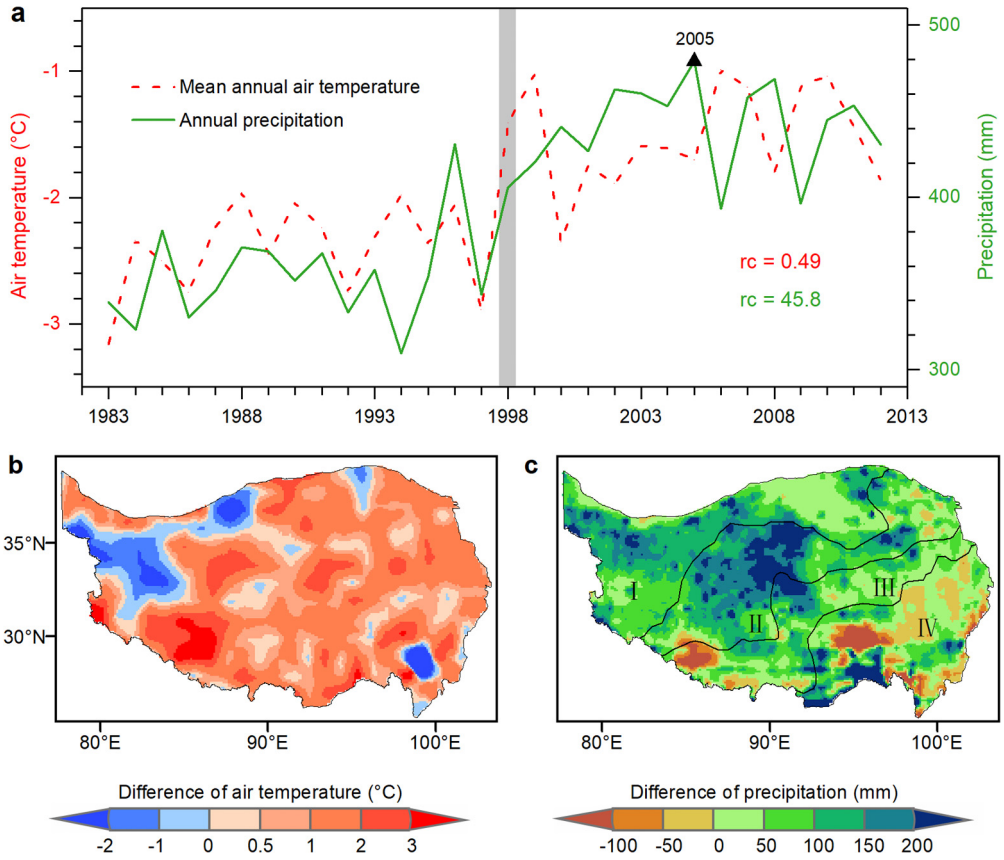

Fig. 1. Variabilities of air temperature and precipitation over the QTP. (a) Time series of mean annual air temperature (MAAT) and annual precipitation (AP) during 1983–2012. Decadal linear trends (denoted by 'rc') are shown by the numbers in the panel. The vertical shading marks the pivotal year 1998. The wettest year is indicated by a triangle. (b) and (c) Difference maps depicting the differences in MAAT and AP between two phases, i.e., 1998–2012 and 1983–1997, respectively. The dry-wet climate divisions in the map (c) is based on the climate classification and the average AP for 1983–2012 on the QTP. I ∼ IV stands for the arid zone (hereinafter AZ), semi-arid zone (SAZ), semi-humid zone (SHZ), humid zone (HZ), respectively. (For interpretation of the colors in the figure(s), the reader is referred to the web version of this article.)

of permafrost. The ALT is determined by linear interpolation between two adjacent depths above and below the 0 °C isotherm to find the maximum depth in the thawed state. Similarly, the TTOP is estimated as an average temperature at the depth of ALT. For simplicity, the ALT and TTOP time series were obtained by averaging over the regions that are simulated as permafrost in the corresponding period under the CTL. The Albers equal-area conic projection was applied to ensure no distortion in calculating permafrost area.

The differences between the results from warming/wetting scenarios and the CTL reflect the effects of temperature/precipitation changes on permafrost. By subtracting the CTL results from the three scenarios, we obtained the differences and drew the corresponding boxplots for the selected indicators. For example, if positive differences in a given indicator are shown in the boxplots for the warming alone scenario, it indicates that air temperature warming exerts positive impacts on that indicator. We also drew spatial difference maps relative to the CTL outcomes. The contributions of one-degree warming and 100 mm wetting to the changes in ALT and TTOP were computed. The contribution of warming/wetting is defined as the ratio of the difference in the indicator mean over the difference in the temperature/precipitation mean.

3. Results and discussion

3.1. Spatiotemporal characteristics of climate warming and wetting over the QTP

The mean annual air temperature (MAAT) over the QTP is characterized by a rapid upward shift during 1983–2012 (red line in Fig. 1a). The warming rate was 0.49 °C/decade, broadly consistent

with site observations. It was about three times greater than the global mean (Duan and Xiao, 2015). Such a rate has never been greater in any past periods on the QTP. The period 1983–2012 was also very likely the warmest 30-year period in the last 800 years in the Northern Hemisphere (IPCC, 2013). In contrast to the global warming hiatus in 1998–2012 (Huang et al., 2017), from 1998 onward steady multi-decadal warming continued to exist over the QTP. The strong El Niño event in the Northern Hemisphere beginning in 1998 was reportedly leading to an increase in global average temperature (Karl et al., 2015). The increasing trend of temperature was particularly evident on the QTP. In comparison to the phase of 1983–1997, the average MAAT in 1998–2012 increased remarkably by 0.89 °C. The difference map of MAAT between the two phases shows warming trends prevailing throughout the entire QTP (Fig. 1b). Widespread positive differences colored in red, i.e., warming trends, can be observed in most regions, except for some small portions in the northwest and southeast QTP where cooling trends were present. Both temporal and spatial patterns indicate that the QTP has experienced prominent warming after 1998.

Unlike prevalent warming that was widely recognized, precipitation change patterns over the QTP appear more complicated. The AP averaged across the QTP was significantly increasing from 1983 to 2012 at a rate of 45.8 mm/decade (green line in Fig. 1a). Especially after 1998, the AP has maintained at a high level with 2005 being the wettest year. The average AP in 1998–2012 was higher by 86 mm than the average of 1983–1997. Abrupt changes around 1998 can be detected by both MAAT and AP. This corroborates with the findings of the same pivotal year in the previous studies (Gao et al., 2014; Kuang and Jiao, 2016; Sun et al., 2020). Precipitation changes between the two phases varied in space (Fig. 1c). It is evident that the spatial differences occurred were mostly positive, implying that most QTP became wetter in the second phase. This wetting correlates with an increase of water vapor convergence due to circulation changes (Zhang et al., 2017). More specifically, the AP intensively increased on the northern QTP, with the largest increase appearing on the central QTP, known as Qiangtang High Plain. In some areas of the southeastern and southern QTP, the AP declined to some extent. By superimposing a dry-wet climate division on the AP distribution (Fig. 1c), it is obvious that the change patterns of AP differed by climate zone. It was becoming wetter in arid and semi-arid zones, whereas relatively drier in some areas of semi-humid and humid zones. In general, the QTP tended to be wetter in the second phase. These results confirm that the QTP has experienced pronounced warming and concomitant wetting since the mid-1990s although there were still regional exceptions.

3.2. Permafrost responses to climate warming and wetting

Fig. 2 illustrates the changes in permafrost indicators (ALT, TTOP, and permafrost area) simulated under three warming/wetting scenarios and the CTL scenario. The results show pronounced distinctions in terms of permafrost responses to warming and/or wetting conditions. Positive differences in ALT, TTOP, and loss of permafrost area relative to the CTL consistently appeared in the warming alone scenario, suggesting that more permafrost degradation had occurred than in the CTL. Meanwhile, persistent negative differences that occurred in the wetting alone scenario indicate that more permafrost has been developed than in the CTL, attributable to more precipitation in the wetting alone scenario than the CTL. In terms of all three indicators, the warming alone curves and the wetting alone curves depart from the CTL curves in an opposite direction. It signifies that permafrost over the QTP has opposite responses to climate warming and wetting. In other words, climate warming thermally degraded permafrost whereas climate wetting favored permafrost formation. Therefore, as expected, the historical scenario with both warming and wetting in place produced in-between results as a consequence of offsetting each other's impacts. Under this scenario, a short-term reversal of all indicators has occurred after 2000, i.e., ALT and TTOP decreased in 2000–2004 and the permafrost area expanded in 2001–2005. It was caused by the joint influences of increased precipitation in 1998–2005 and relatively low MAAT in 2000–2005, as exhibited in Fig. 1a. Alongside the positive role of warming in permafrost degradation, these comparisons reveal that increased precipitation exerts an important role in modulating permafrost thermal regimes.

Spatially, in most areas over the QTP, the trends in terms of the differences in permafrost indicators under the three warming/wetting scenarios (Fig. 3) are consistent with those discovered from the temporal analyses (Fig. 2). To better represent the spatial variations in permafrost area, we used transition of frozen ground type as a proxy indicator. Conversion of previous permafrost into seasonally frozen ground is termed as positive degradation. Positive differences in all indicators against the CTL dominated in the warming alone scenario, while prevalent negative differences were observed in the wetting alone scenario. However, the distributions of positive and negative differences were comparable in the historical scenario. By design, the warming alone scenario represents higher temperature conditions than the CTL. Considerable permafrost degradation has occurred over the QTP in response to a warmer climate than in the CTL, as evidenced by thickened ALTs, higher TTOPs, and extensive permafrost losses across the plateau (top row in Fig. 3), with exceptions in some regions on the northwest QTP that rather affected by regional cooling. Although the visible permafrost degradation was not much in space (Fig. 3g), there was intensive thermal degradation within the permafrost body on the central QTP that is an alpine continuous permafrost region, where ALT and TTOP were simulated to dramatically increase in the warming alone scenario. The spatial patterns obtained for this scenario are highly correlated with the MAAT differences in space (Fig. 1b). In contrast, thinner ALTs, lower TTOPs, and increased permafrost areas were simulated over the most portions of QTP in the wetting alone scenario (middle row in Fig. 3), as more precipitation took place in the wetting alone scenario than the CTL. Moreover, distinct from warming induced patterns, precipitation induced patterns show notable regional differences. The overall spatial patterns broadly match the summer precipitation variabilities in space (Fig. 1c). Because precipitation over the QTP is mostly concentrated in summer with less than 10% in winter (Wang et al., 2018), the spatial variabilities of summer precipitation bear great resemblance to the AP pattern (Fig. 1c). Differing from the fabricated sole factor scenarios, the historical scenario characterizes the conditions of simultaneous warming and wetting relative to the CTL. The coexistence of extensive positive and negative differences in space can be observed (bottom row in Fig. 3). While wetting can offset the impacts of warming, in a certain region one factor might dominate. The most negative differences appeared in the northwest QTP, where the regional cooling and the wetting, both of which are conducive to permafrost formation, multiplied the differences as compared to the CTL. While the most conspicuous thermal offset occurred on the central QTP in Fig. 3d, the impacts of wetting to permafrost in the same region were also huge (Fig. 3e). The consequent differences (Fig. 3f) under the historical scenario remained positive on most central QTP. We can imagine permafrost on the central QTP would have undergone unprecedented thermal degradation in response to climate warming assuming no wetting in the second phase. Therefore, by contrasting the outcomes of three warming/wetting scenarios, it was discovered that climate wetting on the QTP inhibits permafrost thermal degradation when exposed to a warming climate.

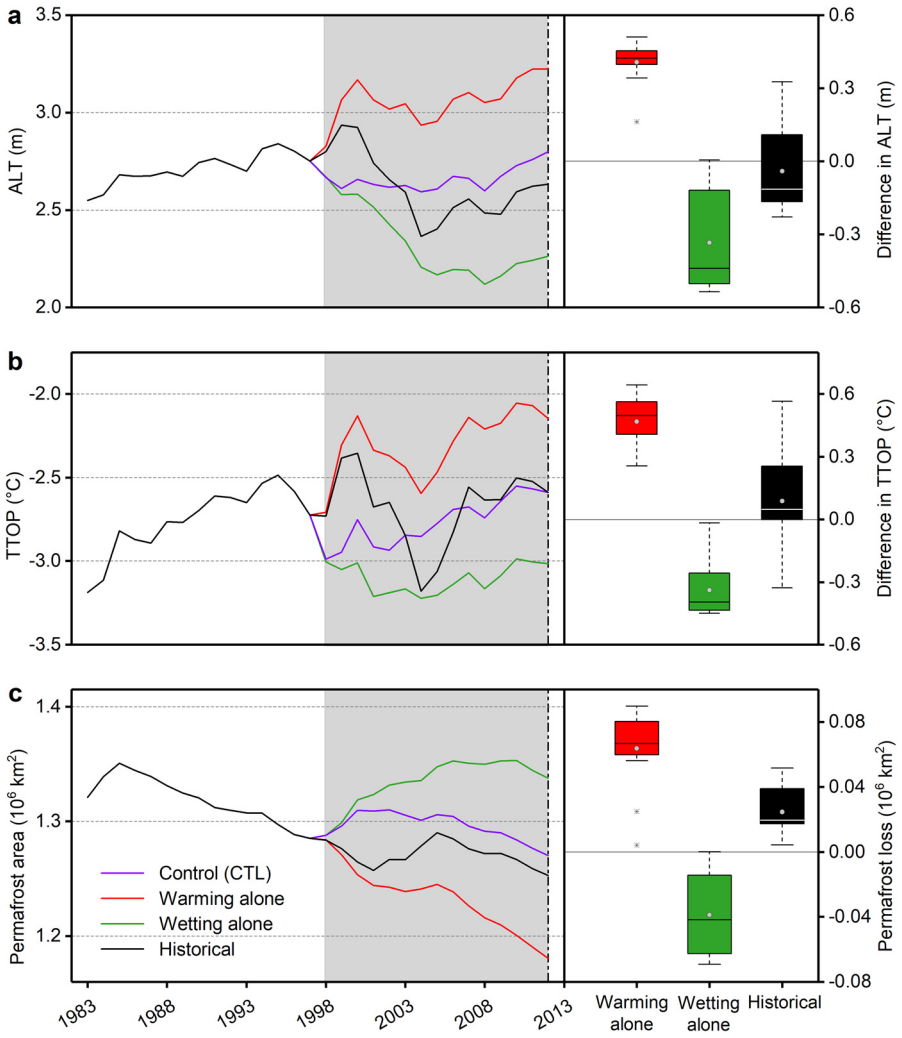

Fig. 2. Changes in permafrost indicator during 1983–2012 under four scenarios. (a) Active layer thickness (ALT) and (b) temperature at the top of permafrost (TTOP) in the permafrost regions, (c) permafrost area. The shaded area marks a contrast period 1998–2012. The control scenario (CTL) serves as a contrast benchmark, representing no warming and wetting between the two phases. The warming/wetting alone scenarios reflect the separated impacts of climate warming/wetting relative to the CTL. The historical scenario represents historical permafrost changes under real climate conditions, which are with both warming and wetting. Differences in ALT, TTOP, and permafrost loss, obtained by subtracting the CTL results from the results of the warming/wetting alone and historical scenarios during 1998–2012, are expressed in the boxplots. The boxes represent 25–75% quartiles and the whiskers are 1.5 interquartile ranges from the medians that are shown in black lines in the boxes. The gray dots indicate mean values, and the star symbol (*) indicates outlier values.

3.3. Permafrost responses to wetting in dry-wet climate zones

We noticed that the spatial patterns for the differences in permafrost indicators under the wetting alone scenario (middle row in Fig. 3) show distinctive regional differences. It is suggestive of differing permafrost responses to wetting in dry-wet climate zones, which to our knowledge has never been reported in previous studies. The most sensitive responses, indicated by the largest negative differences in ALT and TTOP (Fig. 3b and 3e), were found in the arid zone (AZ), followed by the semi-arid zone (SAZ). The AZ and SAZ account for over 60% of the total permafrost area on the QTP, with most of them located in continuous permafrost regions. Despite most of the permafrost in those zones remained stable in type, a lot of seasonally frozen ground in the transition areas has converted into permafrost driven by increased precipitation in this scenario (Fig. 3h). Taken together, these results suggest that the increases in summer precipitation exert very strong cooling effects on frozen ground in the AZ and SAZ. By contrasting the outcomes from the three warming/wetting scenarios, it is clear that the substantially increased precipitation in 1998–2012 prevented massive permafrost degradation resulted from simultaneous climate warming in the AZ and SAZ. Through this simulation, we confirmed the critical role of wetting in regulating permafrost dynamics over the QTP, particularly in the vast AZ and SAZ.

The effects of wetting on frozen ground diminished gradually from dry areas to wet areas. Fig. 4 presents the time series of differences in ATL, TTOP, and summer precipitation (ΔP_s) for the four dry-wet zones. The differences were computed by subtracting the CTL results from the wetting alone scenario. The more divergence from the zero horizontal line, the more impacts received from wetting. Both ALT and TTOP vary considerably in response to the changed summer precipitation in the four zones. The most obvious cooling effect was observed in the AZ, where ALT and TTOP declined substantially. With ΔP_s increasing progressively, the negative differences for ALT and TTOP became larger and the maxima were reached in the wettest year 2005. When ΔP_s exceeded 100 mm, the cooling effect basically stopped growing in the AZ. The effect was less intense in the SAZ even though ΔP_s in this zone became greater than in the AZ after 2005. Therefore, the strength of the cooling effect depends on not only the amount of increased precipitation, but more importantly the dry-wet zone where permafrost underlies. In the SHZ, ΔP_s continued to increase

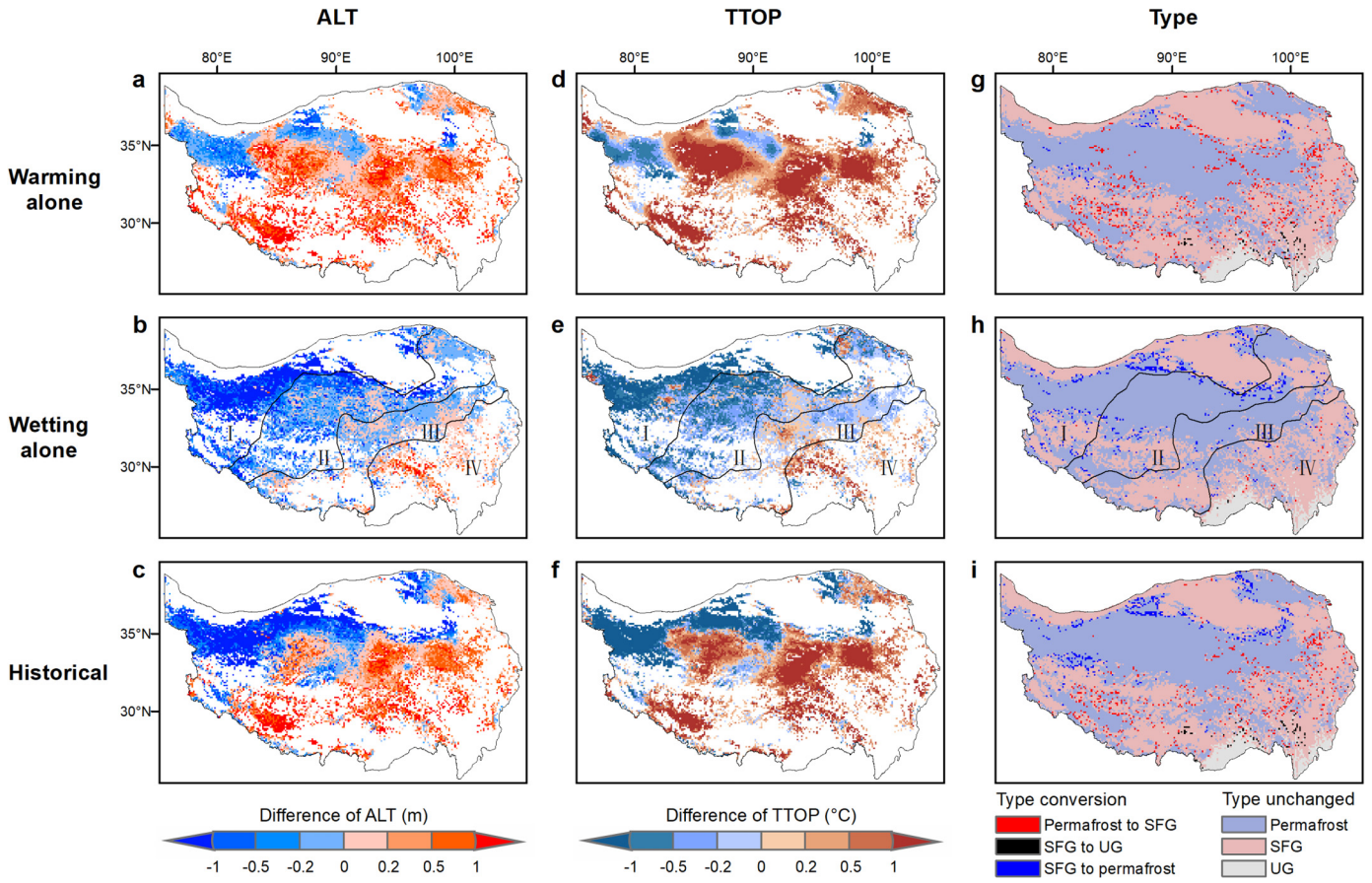

Fig. 3. Spatial difference maps for 2012, showing the differences in (a ∼ c) ALT and (d ∼ f) TTOP in the permafrost regions for the warming/wetting alone and historical scenarios by subtracting the CTL results from each scenario results. The dark blue indicates the largest negative differences against the CTL and the red represents positive differences. (g ∼ i) Type transition maps of frozen ground in 2012, showing the conversion of the type in the CTL result into the types in other three warming/wetting scenarios. SFG = seasonally frozen ground, UG = unfrozen ground. The wetting alone maps contain four dry-wet zones, in which I ∼ IV stands for AZ, SAZ, SHZ, and HZ, respectively.

over time with a magnitude less than in AZ and SAZ, the cooling effect on permafrost was rather mild. Unlike the three zones, ΔP_S in the HZ oscillated around the zero line with a generally declining trend over the study period. As a result, small positive differences in ALT and TTOP, contrary to those in the other three zones, were found in the HZ. The trends between permafrost indicators and ΔP_S are negatively correlated. From these results, it can be concluded the increases in summer precipitation exert strong cooling effects on permafrost thermal regime and slow down thermal degradation in arid and semi-arid areas, whereas in humid or semi-humid areas the effects are rather limited or even opposite.

3.4. Quantification of permafrost responses to warming and wetting

The impacts of warming and wetting on permafrost thermal indicators (ALT and TTOP) were quantified as listed in Table 2. As the impacts of wetting vary in climate zones, the quantification was also made for each zone separately. The results show, the ALT increases by 0.46 m and the TTOP by 0.53 °C in response to an average of one degree increase in air temperature in the permafrost regions over the QTP. Taking the QTP as a whole, wetting with 100 mm more summer precipitation results in a reduction of the ALT by 0.35 m and the TTOP by 0.36 °C. In the AZ, the ALT declines by as much as 0.75 m and the TTOP by 0.71 °C, in response to additional 100 mm summer precipitation. In the SAZ and SHZ, the reductions are less, i.e., 0.24 m in ALT and 0.22 °C in TTOP for the SAZ, and 0.10 m and 0.19 °C for the SHZ. Note that the difference of summer precipitation in the HZ was minimal between the post-phase and the pre-phase, and the HZ covers a small fraction (∼14%) of the total permafrost area, most of which is of the type of island permafrost. Thus, we excluded the HZ from quantifying contributions. Obviously, the strongest responses of wetting occur in the AZ, and the next is in the SAZ. The quantification confirms that while climate warming induces permafrost thermal degradation over most parts of the QTP, the concomitant wetting can effectively reverse the degradation in dry areas (AZ and SAZ).

3.5. Mechanisms of the effects of climate wetting on permafrost

In cold and dry permafrost areas, precipitation as a major source of soil moisture can alter soil thermal regimes (Lupascu et al., 2014). Percolating rainfall delivers heat to the depth, influencing thermal and hydrological processes in the active layer and permafrost. Our modeling studies show that increases in summer precipitation have strong cooling effects on permafrost thermal dynamics in arid and semi-arid areas, as evidenced by remarkable declines in ALT and TTOP (Fig. 3 and 4). This may be explained by accompanying heat exchanges when rainfall reaches the soil surface, infiltrates and percolates to the deep soils. More precipitation increases soil surface wetness and soil moisture, leading to increasing soil surface evaporation, which consumes heat energy and reduces the amount of heat transporting to the deep. Rainfall heat exchanges with the surrounding soils in a form of convection. At the time when phase changes are occurring within the active layer, heat transfer will be tremendously increased by heat convection. Meanwhile, increased soil moisture can absorb abun-

Table 2
Contributions of one-degree warming and 100 mm wetting in permafrost regions to the changes in ALT and TTOP.

Climatic change	Zones	Contributions to indicators		Historical increments $\triangle(.) = (.)_{post} - (.)_{pre}$
		ALT (m/100 mm)	TTOP (°C/100 mm)	$\triangle\overline{P}_s$ (mm)
Wetting	Arid	−0.75	−0.71	110
	Semi-arid	−0.24	−0.22	127
	Semi-humid	−0.10	−0.19	68
	Humid	–	–	6
	Mean	−0.35	−0.36	93
Warming		ALT (m/°C)	TTOP (°C/°C)	$\triangle\overline{T}$ (°C)
	Mean	0.46	0.53	0.89

Note: The invalid quantifies for the humid zone are indicated by the symbol (–). $\triangle(.) = (.)_{post} - (.)_{pre}$ represents average increments between two phases, and the subscripts pre and post represent pre-phase (1983–1997) and post-phase (1998–2012), respectively. $\triangle\overline{P}_s$ and $\triangle\overline{T}$ represent the averaged increments of P_s and MAAT in post-phase relative to pre-phase, respectively.

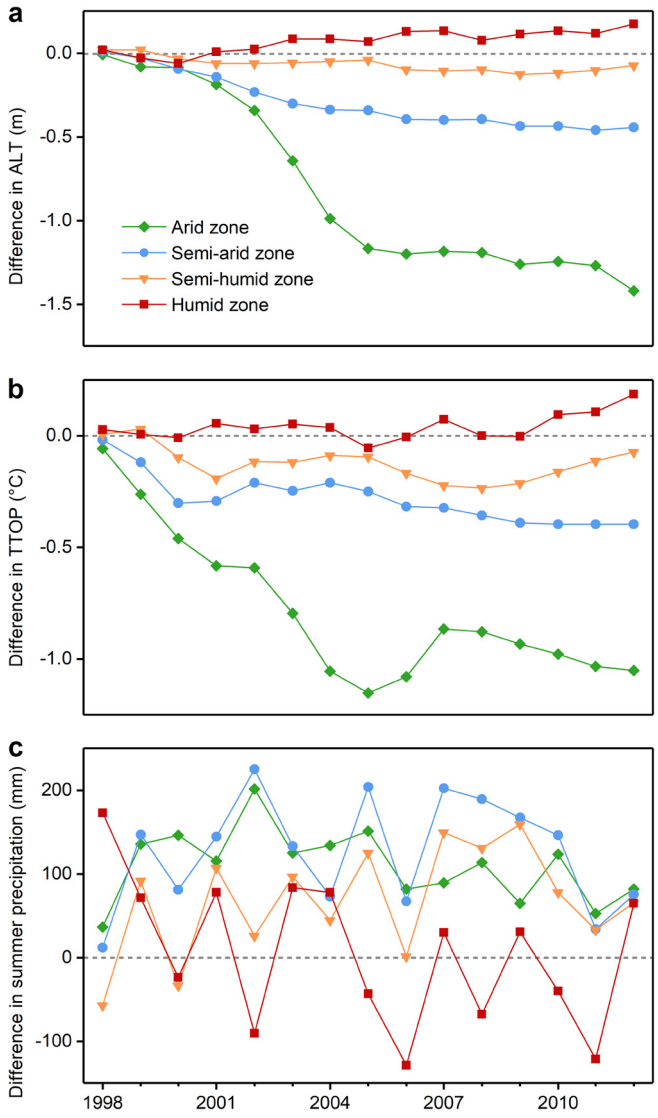

Fig. 4. Differences in the (a) ALT, (b) TTOP, and (c) summer precipitation between the results from the wetting alone scenario and the CTL in the four dry-wet zones during 1998–2012.

dant heat as liquid water has a high specific heat capacity and diminish heat transfer to the deep. When heat is consumed more by evaporating and percolating liquid water than that transferring to soils, it will put a cooling effect on permafrost. As simulated in this study, the cooling effect prevails in arid zones. Such effect of precipitation on permafrost has been already reported in some previous observation-based studies such as Zhang et al. (2001). Our modeling study, from a regional perspective rather than a point perspective as in previous studies, confirms the cooling effects that abundant precipitation may bring to mountainous permafrost, and more importantly, highlights the spatial variability of cooling effects in dry-wet climate zones, with being most prominent in arid and semi-arid zones.

However, when a large amount of rainfall percolates into the deeper soils, it may cause an opposite, warming effect on permafrost. Summer rainfall usually comes with higher temperature than in the deep soils and the convection will effectively increase the soil temperature when the liquid percolates through the soil. Even if we do not consider the convective heat transfer as in the Noah LSM, more liquid water accumulating at the bottom of the active layer will alter the process of phase change occurring there. In the freezing period, bidirectional freezing will take place. The upward freezing occurs at the interface between the thawing soils and permafrost and this process will release massive latent heat, thus affecting the thermal regime of the permafrost body. The Noah LSM assumes the liquid water holds the temperature equal to the ambient soils. Therefore, after heavy rainfall rapidly reaches the base of the active layer in summer, those extra water contents will serve to warm the permafrost body during the subsequent freezing period. It is liable to occur in the event of heavy rainfalls in summer. In the semi-arid areas over the QTP (Fig. 5d), we observed in our simulations the presence of higher soil temperatures at deeper soils (6 m and 10 m) in the wettest year of 2005 under the wetting alone scenario (Fig. 5a and 5b), while conversely both ALT and TTOP measured at a relatively shallow depth (2.5 m on average) were simulated to be reduced. By examining the driving forces, the warming effect is related to the occurrence of heavy summer precipitation in the semi-arid zones (Fig. 5c). It implies the existence of dual effects on permafrost in semi-arid areas, i.e., a cooling effect in shallow depths and a warming effect in deep depths. The warming effect of excessive precipitation can be supported by some permafrost site observations (Luo et al., 2016), where soil temperatures have increased while no apparent local warming trends were found. Luo et al. (2016) attributed the warming permafrost to increasing summer precipitation. A similar finding was also provided by a simulation work performed by Subin et al. (2013). These findings together provide evidence that increasing summer precipitation in semi-arid high altitudes is likely to have dual effects on permafrost thermal regimes.

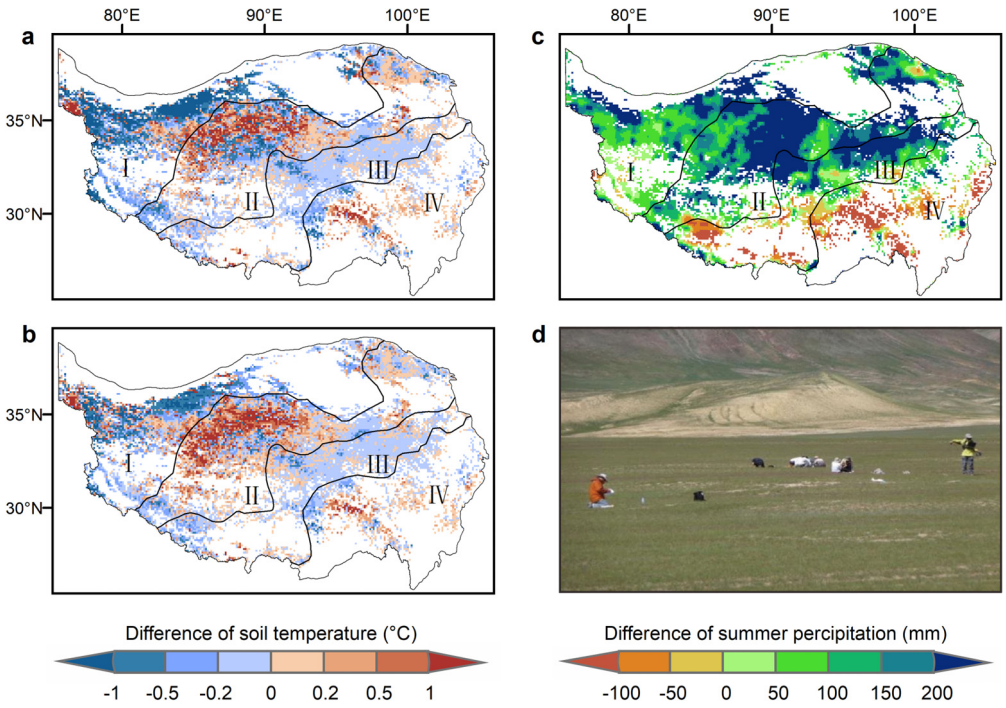

Fig. 5. Difference maps of the wettest year (2005) between the wetting alone scenario and the CTL, showing the differences in permafrost soil temperature at (a) 6 m and (b) 10 m depth and (c) summer precipitation in permafrost regions. Dark blue and crimson indicate the largest negative and positive differences, respectively. I ∼ IV stands for AZ, SAZ, SHZ, and HZ. (d) A picture showing the permafrost landscape in the SAZ over the QTP, reproduced from Zhou et al. (2015).

Through our experiments, it can be found that the cooling effect by increasing precipitation is not obvious in relatively wet areas. However, permafrost in dry areas is more susceptible to wetting. As such, future wetting could mitigate permafrost responses to climate warming. The complication behind the mechanisms calls for more in situ observation as well as theoretical studies towards understanding and assessing the vulnerability of permafrost to future climate warming and wetting. The Noah LSM used in this study is limited in the lack of considering convective heat transfer and the role of convection in exchanging heat in a freeze-thaw cycle is worthy to further study. In addition, the current study is based on a single driving dataset. The uncertainties associated with the driving data and model parameters, in particular, the soil parameters, may bias the results.

4. Conclusions

This study provides a new perspective on permafrost responses to climatic warming and wetting through numerical experiments. From the results, we have drawn the following conclusions. The QTP has experienced pronounced warming and wetting especially after the mid-1990s. Permafrost over the QTP has opposite responses to climate warming and wetting. While climatic warming leads to permafrost thermal degradation over the QTP, wetting prevents from the degradation, especially in the vast arid and semi-arid areas. The increases in summer precipitation exert strong cooling effects on permafrost thermal regimes in arid and semi-arid areas, whereas in wet areas the effect is rather little. It was estimated that one-degree warming of air temperature in permafrost regions of QTP leads to an increase of 0.46 m in ALT and 0.53 °C in TTOP. An increase of 100 mm in summer precipitation causes a mean reduction of 0.35 m in ALT and 0.36 °C in TTOP. Regional differences are remarkable in terms of permafrost responses to wetting. The largest decrease of 0.75 m in ALT and 0.71 °C in TTOP in response to 100 mm additional summer precipitation occurred in the arid zone, followed by 0.24 m and 0.22 °C in the semi-arid zone, 0.10 m and 0.19 °C in the semi-humid zone. We also found that increased summer precipitation in semi-arid high altitudes has dual effects on permafrost dynamics. When heavy summer rainfall occurs in those areas, it imposes a cooling effect on the active layer and a warming effect on the underlying permafrost body. As shown by the experimental simulations, apart from climatic warming, wetting is also a critical factor regulating the current thermal regimes of permafrost over the QTP and it will become even more important when precipitation has been projected to continuously increase in the future. Insights into these aspects are expected to contribute a better understanding of the roles of warming and wetting in altering permafrost thermal responses.

CRediT authorship contribution statement

G.Z. conceptualized this research, performed simulations, analyzed data, and wrote the original draft. Z.N. conceived the idea, supervised the study, reviewed, and edited the manuscript. Y.L. and G.Z. conducted climatic zonation. L.Z. and G.C. provided very valuable suggestions for this paper. All authors reviewed and accepted the manuscript.

Declaration of competing interest

The authors declare that they have no known competing financial interests or personal relationships that could have appeared to influence the work reported in this paper.

Acknowledgements

The authors wish to express their thanks for the financial support of the Second Tibetan Plateau Scientific Expedition and Research (STEP) program (2019QZKK0905-08) from Ministry of Science and Technology of the People's Republic of China, and the National Natural Science Foundation of China (41931180, 41971074). We thank the National Tibetan Plateau Data Center (http://data.tpdc.ac.cn) and the National Cryosphere Desert Data

Center (http://crensed.ac.cn) for providing data. The results and associated data in this study can be obtained from the OSF storage (https://doi.org/10.17605/osf.io/grdb8).

References

Biskaborn, B.K., Smith, S.L., Noetzli, J., Matthes, H., Vieira, G., Streletskiy, D.A., et al., 2019. Permafrost is warming at a global scale. Nat. Commun. 10 (1), 264. https://doi.org/10.1038/s41467-018-08240-4.

Cai, H., Jin, L., Li, Y., Li, F., Han, L., 2018. Influence of precipitation on permafrost in Fenghuo Mountain region of Tibetan Plateau. J. China Railw. Soc. 40 (9), 104–110. https://doi.org/10.3969/j.issn.1001-8360.2018.09.015 (in Chinese).

Chen, F., Janjić, Z., Mitchell, K., 1997. Impact of atmospheric surface-layer parameterizations in the new land-surface scheme of the NCEP mesoscale eta model. Bound.-Layer Meteorol. 85 (3), 391–421. https://doi.org/10.1023/A:1000531001463.

Chen, H., Nan, Z., Zhao, L., Ding, Y., Chen, J., Pang, Q., 2015. Noah modelling of the permafrost distribution and characteristics in the West Kunlun area, Qinghai-Tibet Plateau, China. Permafr. Periglac. Process. 26 (2), 160–174. https://doi.org/10.1002/ppp.1841.

Chen, Y., Yang, K., Zhou, D., Qin, J., Guo, X., 2010. Improving the Noah land surface model in arid regions with an appropriate parameterization of the thermal roughness length. J. Hydrometeorol. 11 (4), 995–1006. https://doi.org/10.1175/2010JHM1185.1.

Chen, Y., Yang, K., He, J., Qin, J., Shi, J., Du, J., et al., 2011. Improving land surface temperature modeling for dry land of China. J. Geophys. Res. 116 (D20), D20104. https://doi.org/10.1029/2011JD015921.

Cheng, G., 2004. Influences of local factors on permafrost occurrence and their implications for Qinghai-Xizang Railway design. Sci. China, Ser. D, Earth Sci. 47 (8), 704–709. https://doi.org/10.1007/BF02893300.

Cheng, G., Wu, T., 2007. Responses of permafrost to climate change and their environmental significance, Qinghai-Tibet Plateau. J. Geophys. Res. 112 (F2), F2S–F3S. https://doi.org/10.1029/2006JF000631.

Cheng, G., Zhao, L., Li, R., Wu, X., Sheng, Y., Hu, G., et al., 2019. Characteristic, changes and impacts of permafrost on Qinghai-Tibet Plateau. Chin. Sci. Bull. 64 (27), 2783–2795. https://doi.org/10.1360/TB-2019-0191 (in Chinese).

Duan, A., Xiao, Z., 2015. Does the climate warming hiatus exist over the Tibetan Plateau? Sci. Rep. 5 (1), 13711. https://doi.org/10.1038/srep13711.

Ek, M.B., Mitchell, K.E., Lin, Y., Rogers, E., Grunmann, P., Koren, V., et al., 2003. Implementation of Noah land surface model advances in the National Centers for Environmental Prediction operational mesoscale Eta model. J. Geophys. Res., Atmos. 108 (D22), 8851. https://doi.org/10.1029/2002JD003296.

Gao, Y., Cuo, L., Zhang, Y., 2014. Changes in moisture flux over the Tibetan Plateau during 1979–2011 and possible mechanisms. J. Climate 27 (5), 1876–1893. https://doi.org/10.1175/JCLI-D-13-00321.1.

Gao, Y., Li, X., Ruby Leung, L., Chen, D., Xu, J., 2015. Aridity changes in the Tibetan Plateau in a warming climate. Environ. Res. Lett. 10 (3), 34013. https://doi.org/10.1088/1748-9326/10/3/034013.

Gao, Y., Xiao, L., Chen, D., Xu, J., Zhang, H., 2017. Comparison between past and future extreme precipitations simulated by global and regional climate models over the Tibetan Plateau. Int. J. Climatol. 38 (3), 1285–1297. https://doi.org/10.1002/joc.5243.

He, J., Yang, K., Tang, W., Lu, H., Qin, J., Chen, Y., et al., 2020. The first high-resolution meteorological forcing dataset for land process studies over China. Sci. Data 7 (1). https://doi.org/10.1038/s41597-020-0369-y.

Huang, J., Zhang, X., Zhang, Q., Lin, Y., Hao, M., Luo, Y., et al., 2017. Recently amplified Arctic warming has contributed to a continual global warming trend. Nat. Clim. Change 7 (12), 875–879. https://doi.org/10.1038/s41558-017-0009-5.

IPCC, 2013. Climate Change 2013: The Physical Science Basis, Contribution of Working Group I to the Fifth Assessment Report of the Intergovernmental Panel on Climate Change. Cambridge University Press, Cambridge. 1535 pp.

Kang, S., Xu, Y., You, Q., Flügel, W., Pepin, N., Yao, T., 2010. Review of climate and cryospheric change in the Tibetan Plateau. Environ. Res. Lett. 5 (1), 15101. https://doi.org/10.1088/1748-9326/5/1/015101.

Karl, T.R., Arguez, A., Huang, B., Lawrimore, J.H., McMahon, J.R., Menne, M.J., et al., 2015. Possible artifacts of data biases in the recent global surface warming hiatus. Science 348 (6242), 1469–1472. https://doi.org/10.1126/science.aaa5632.

Koven, C.D., Bruno, R., Pierre, F., Philippe, C., Patricia, C., Dmitry, K., et al., 2011. Permafrost carbon-climate feedbacks accelerate global warming. Proc. Natl. Acad. Sci. 108 (36), 14769–14774. https://doi.org/10.1073/pnas.1103910108.

Kuang, X., Jiao, J.J., 2016. Review on climate change on the Tibetan Plateau during the last half century. J. Geophys. Res., Atmos. 121 (8), 3979–4007. https://doi.org/10.1002/2015JD024728.

Lei, Y., Yang, K., Wang, B., Sheng, Y., Bird, B.W., Zhang, G., et al., 2014. Response of inland lake dynamics over the Tibetan Plateau to climate change. Clim. Change 125 (2), 281–290. https://doi.org/10.1007/s10584-014-1175-3.

Li, D., Wen, Z., Cheng, Q., Xing, A., Zhang, M., Li, A., 2019. Thermal dynamics of the permafrost active layer under increased precipitation at the Qinghai-Tibet Plateau. J. Mt. Sci. 16 (2), 309–322. https://doi.org/10.1007/s11629-018-5153-5.

Li, L., Yang, S., Wang, Z., Zhu, X., Tang, H., 2010. Evidence of warming and wetting climate over the Qinghai-Tibet Plateau. Arct. Antarct. Alp. Res. 42 (4), 449–457. https://doi.org/10.1657/1938-4246-42.4.449.

Liu, X., Chen, B., 2000. Climatic warming in the Tibetan Plateau during recent decades. Int. J. Climatol. 20 (14), 1729–1742. https://doi.org/10.1002/1097-0088(20001130)20:14<1729::AID-JOC556>3.0.CO;2-Y.

Luo, S., Fang, X., Lyu, S., Ma, D., Chang, Y., Song, M., et al., 2016. Frozen ground temperature trends associated with climate change in the Tibetan Plateau Three River Source Region from 1980 to 2014. Clim. Res. 67 (3), 241–255. https://doi.org/10.3354/cr01371.

Lupascu, M., Welker, J.M., Seibt, U., Maseyk, K., Xu, X., Czimczik, C.I., 2014. High Arctic wetting reduces permafrost carbon feedbacks to climate warming. Nat. Clim. Change 4 (1), 51–55. https://doi.org/10.1038/nclimate2058.

Mahrt, L., Ek, M., 1984. The influence of atmospheric stability on potential evaporation. J. Clim. Appl. Meteorol. 23 (2), 222–234. https://doi.org/10.1175/1520-0450(1984)023<0222:TIOASO>2.0.CO;2.

Niu, T., Chen, L., Zhou, Z., 2004. The characteristics of climate change over the Tibetan Plateau the last 40 years and the detection of climatic jumps. Adv. Atmos. Sci. 21 (2), 193–203. https://doi.org/10.1007/BF02915705.

Ran, Y., Li, X., Cheng, G., 2018. Climate warming over the past half century has led to thermal degradation of permafrost on the Qinghai–Tibet Plateau. Cryosphere 12 (2), 595–608. https://doi.org/10.5194/tc-12-595-2018.

Subin, Z.M., Koven, C.D., Riley, W.J., Torn, M.S., Lawrence, D.M., Swenson, S.C., 2013. Effects of soil moisture on the responses of soil temperatures to climate change in cold regions*. J. Climate 26 (10), 3139–3158. https://doi.org/10.1175/JCLI-D-12-00305.1.

Sun, J., Yang, K., Guo, W., Wang, Y., He, J., Lu, H., 2020. Why has the inner Tibetan Plateau become wetter since the mid-1990s? J. Climate 33 (19), 8507–8522. https://doi.org/10.1175/JCLI-D-19-0471.1.

van der Velde, R., Su, Z., Ek, M., Rodell, M., Ma, Y., 2009. Influence of thermodynamic soil and vegetation parameterizations on the simulation of soil temperature states and surface fluxes by the Noah LSM over a Tibetan plateau site. Hydrol. Earth Syst. Sci. 13 (6), 759–777. https://doi.org/10.5194/hess-13-759-2009.

Wang, X., Pang, G., Yang, M., 2018. Precipitation over the Tibetan Plateau during recent decades: a review based on observations and simulations. Int. J. Climatol. 38 (3), 1116–1131. https://doi.org/10.1002/joc.5246.

Wen, Z., Niu, F., Yu, Q., Wang, D., Feng, W., Zheng, J., 2014. The role of rainfall in the thermal-moisture dynamics of the active layer at Beiluhe of Qinghai-Tibetan Plateau. Environ. Earth Sci. 71 (3), 1195–1204. https://doi.org/10.1007/s12665-013-2523-8.

Wu, Q., Hou, Y., Yun, H., Liu, Y., 2015. Changes in active-layer thickness and near-surface permafrost between 2002 and 2012 in Alpine ecosystems, Qinghai–Xizang (Tibet) Plateau, China. Glob. Planet. Change 124, 149–155. https://doi.org/10.1016/j.gloplacha.2014.09.002.

Wu, X., Nan, Z., Zhao, S., Zhao, L., Cheng, G., 2018. Spatial modeling of permafrost distribution and properties on the Qinghai-Tibet Plateau. Permafr. Periglac. Process. 29 (2), 86–99. https://doi.org/10.1002/ppp.1971.

Yang, K., Wu, H., Qin, J., Lin, C., Tang, W., Chen, Y., 2014. Recent climate changes over the Tibetan Plateau and their impacts on energy and water cycle: a review. Glob. Planet. Change 112, 79–91. https://doi.org/10.1016/j.gloplacha.2013.12.001.

Yang, K., Lu, H., Yue, S., Zhang, G., Lei, Y., La, Z., et al., 2018. Quantifying recent precipitation change and predicting lake expansion in the Inner Tibetan Plateau. Clim. Change 147, 149–163. https://doi.org/10.1007/s10584-017-2127-5.

Yao, T., Thompson, L., Yang, W., Yu, W., Gao, Y., Guo, X., et al., 2012. Different glacier status with atmospheric circulations in Tibetan Plateau and surroundings. Nat. Clim. Change 2 (9), 663–667. https://doi.org/10.1038/nclimate1580.

Yao, T., Xue, Y., Chen, D., Chen, F., Thompson, L., Cui, P., et al., 2019. Recent third pole's rapid warming accompanies cryospheric melt and water cycle intensification and interactions between monsoon and environment: multidisciplinary approach with observations, modeling, and analysis. Bull. Am. Meteorol. Soc. 100 (3), 423–444. https://doi.org/10.1175/BAMS-D-17-0057.1.

Zhang, G., Nan, Z., Wu, X., Ji, H., Zhao, S., 2019. The role of winter warming in permafrost change over the Qinghai-Tibet Plateau. Geophys. Res. Lett. 46 (20), 11261–11269. https://doi.org/10.1029/2019GL084292.

Zhang, T., Barry, R.G., Gilichinsky, D., Bykhovets, S.S., Sorokovikov, V.A., Ye, J., 2001. An amplified signal of climatic change in soil temperatures during the last century at Irkutsk, Russia. Clim. Change 49, 41–76. https://doi.org/10.1023/A:1010790203146.

Zhang, W., Zhou, T., Zhang, L., 2017. Wetting and greening Tibetan Plateau in early summer in recent decades. J. Geophys. Res., Atmos. 122 (11), 5808–5822. https://doi.org/10.1002/2017JD026468.

Zheng, D., van der Velde, R., Su, Z., Wen, J., Wang, X., 2017. Assessment of Noah land surface model with various runoff parameterizations over a Tibetan river. J. Geophys. Res., Atmos. 122 (3), 1488–1504. https://doi.org/10.1002/2016JD025572.

Zhong, L., Su, Z., Ma, Y., Salama, M.S., Sobrino, J.A., 2011. Accelerated changes of environmental conditions on the Tibetan Plateau caused by climate change. J. Climate 24 (24), 6540–6550. https://doi.org/10.1175/JCLI-D-10-05000.1.

Zhou, C., Zhao, P., Chen, J., 2019. The interdecadal change of summer water vapor over the Tibetan Plateau and associated mechanisms. J. Climate 32 (13), 4103–4119. https://doi.org/10.1175/JCLI-D-18-0364.1.

Zhou, Z., Yi, S., Chen, J., Ye, B., Sheng, Y., Wang, G., et al., 2015. Responses of Alpine grassland to climate warming and permafrost thawing in two basins with different precipitation regimes on the Qinghai-Tibetan Plateaus. Arct. Antarct. Alp. Res. 47 (1), 125–131. https://doi.org/10.1657/AAAR0013-098.

Zhu, X., Wu, T., Li, R., Xie, C., Hu, G., Qin, Y., et al., 2017. Impacts of summer extreme precipitation events on the hydrothermal dynamics of the active layer in the Tanggula permafrost region on the Qinghai-Tibetan Plateau. J. Geophys. Res., Atmos. 122 (21), 511–549. https://doi.org/10.1002/2017JD026736. 567.

Zimov, S.A., Schuur, E.A., Chapin, F.R., 2006. Permafrost and the global carbon budget. Science 312 (5780), 1612–1613. https://doi.org/10.1126/science.1128908.